

Diffraction of radio-frequency waves by plasma turbulence in the edge of a tokamak (*)

S. I. Valvis¹, A. D. Papadopoulos¹, K. Hizanidis¹, P. Papagiannis¹, C. Tsironis¹, A. K. Ram²

¹ National Technical University of Athens, Athens, Greece

² Plasma Science and Fusion Center, MIT, Cambridge MA, USA

(a) Abstract

The Mie-Lorenz-Debye theory of scattering of radio frequency waves (RF) by filamentary structures in the edge of a tokamak plasma has been established in prior publications [1-4]. These results have been verified [5]. Theory and computations show that RF can be reflected, refracted, and diffracted by turbulence. Furthermore, the filamentary structures lead to side scattering of waves and excitation of wave modes different from the launched RF. It is important to quantify the overall effect of turbulence on the propagation of RF since efficiency of heating and current drive by RF waves depends upon the wave characteristics. The commonly used RF ranges vary from the low frequency ion-cyclotron (IC) waves, to medium frequency lower-hybrid (LH) waves, to high-frequency electron cyclotron (EC) waves with wavelengths respectively, large, comparable, or smaller than the radial dimensions of the filaments. Currently, we discuss the scattering as well as the forces exerted by different RF in the edge plasma. Also, we present a code for 3D full wave scattering analysis of arbitrary tensor permittivity and plasma density profiles. The study is applicable to ITER-like plasmas, as well as to plasmas in medium sized tokamaks such as TCV, ASDEX-U and DIII-D and high field concepts like SPARC.

(b) Analytical theory

If we consider the turbulent cylindrical filament of infinite length in z direction, parallel to the externally imposed magnetic field in homogeneous and cold plasma, after an appropriate analysis [3] for the electric field and the magnetic field respectively, one obtains:

$$\tilde{\mathbf{e}}(\rho, \varphi)_{(FI, SC)} = \sum_{M=0, X} \sum_{m=-\infty}^{m=\infty} i^m e^{im\varphi} \left[\mathcal{E}_{mr}^M(\rho) \hat{\mathbf{r}} + \mathcal{E}_{m\varphi}^M(\rho) \hat{\mathbf{\varphi}} + \mathcal{E}_{mz}^M(\rho) \hat{\mathbf{z}} \right]_{(FI, SC)} \quad (1)$$

$$\tilde{\mathbf{h}}(\rho, \varphi)_{(FI, SC)} = \frac{E_0}{H_0} \sqrt{\frac{\epsilon_0}{\mu_0}} \sum_{M=0, X} \sum_{m=-\infty}^{m=\infty} i^m e^{im\varphi} \left[\mathcal{H}_{mr}^M(\rho) \hat{\mathbf{r}} + \mathcal{H}_{m\varphi}^M(\rho) \hat{\mathbf{\varphi}} + \mathcal{H}_{mz}^M(\rho) \hat{\mathbf{z}} \right]_{(FI, SC)} \quad (2)$$

(*SC*: scattered field, *FI*: field inside the filament) where $\mathcal{E}_{mr}^M(\rho)$, $\mathcal{E}_{m\phi}^M(\rho)$, $\mathcal{E}_{mz}^M(\rho)$, $\mathcal{H}_{mr}^M(\rho)$, $\mathcal{H}_{m\phi}^M(\rho)$ and $\mathcal{H}_{mz}^M(\rho)$ are functions only of ρ . The expressions for the incident field are similar, but the first sum of equations (1) and (2) is missing. The results are z independent because the cylinder has infinite length. The parallel to the cylinder axis wave vector component stays the same for all regions. The Poynting vector is calculated as:

$$\tilde{\mathbf{s}} = \frac{1}{2} \operatorname{Re}\{\tilde{\mathbf{e}} \times \tilde{\mathbf{h}}^*\} \quad (3)$$

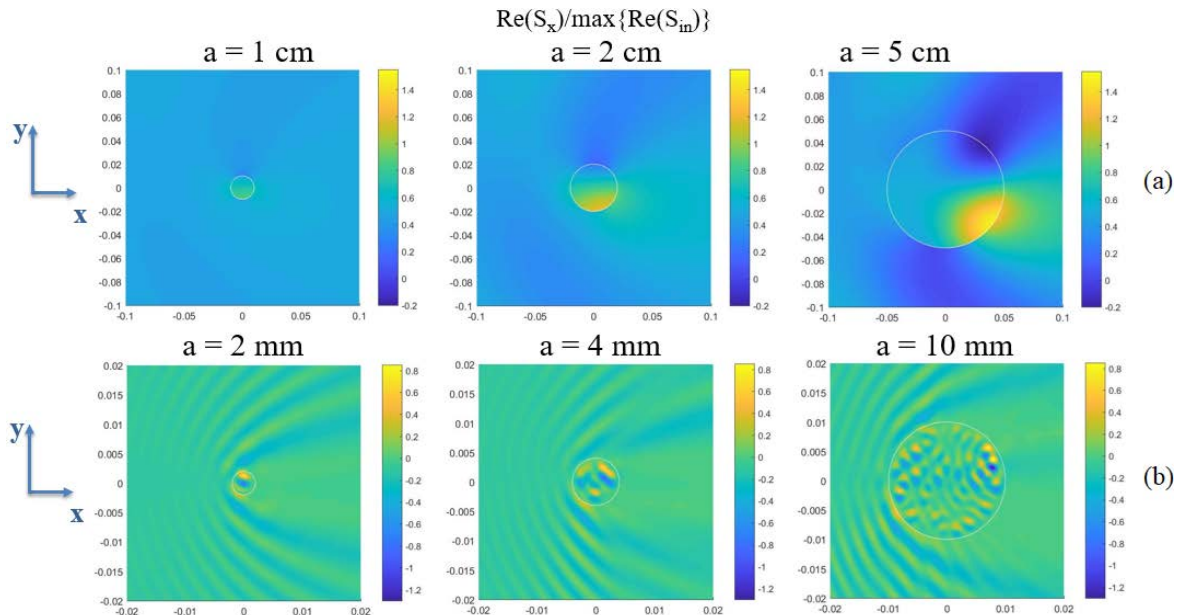
Also, the forces exerted on the cylinder can be calculated from the Maxwell's stress tensor and after an appropriate analysis, for the time averaged normalized radial stress one obtains:

$$\frac{cT_r}{|\tilde{\mathbf{s}}|} = \frac{(K_\rho^{(f)} - K_\rho^{(a)})|p_\phi|^2 + (K_z^{(f)} - K_z^{(a)})|p_z|^2 + (K_\rho|p_r|^2)^{(a)} - (K_\rho|p_r|^2)^{(f)}}{2|\tilde{\mathbf{s}}|} \quad (4)$$

Where in the right side of (4) one can see the elements of the permittivity tensor for the filament (f) and the ambient plasma (a) and the polarizations of the wave.

(c) Scattering results for Ion Cyclotron, Lower Hybrid and Electron Cyclotron plane waves

One can see results for the Poynting vector in the forward direction for IC waves in Figure 1a, LH waves in Figure 1b and EC waves in Figures 1c for plane wave scattering by a single filament, for different radii (a): IC: $a = 1$ cm, 2 cm and 5 cm, LH: $a = 2$ mm, 4 mm and 10 mm, EC: $a = 1.5$ mm, 2.5 mm and 5.0 mm (in figures, units in axes are in meters).



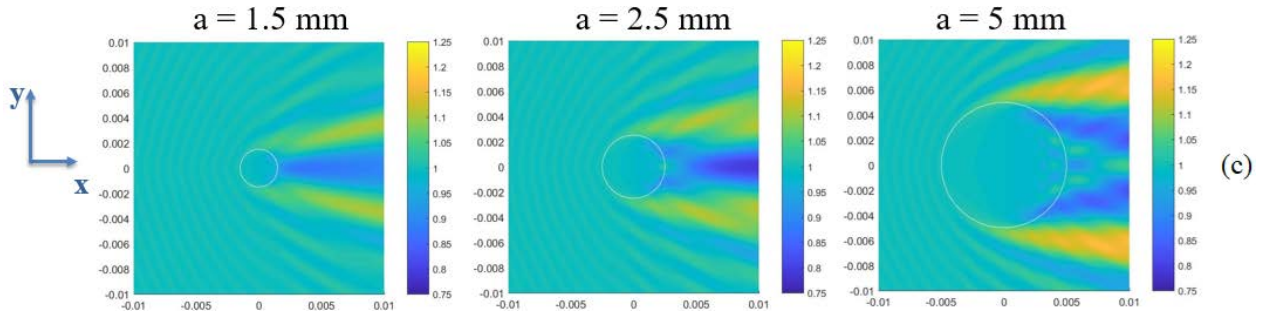


Figure 1: Poynting vector in the forward direction: (a) $f = 120$ MHz (IC), $\lambda = 18.2$ cm, incident polarization: X-mode, $n_{e(\text{ambi})} = 4 \times 10^{19} \text{ m}^{-3}$, $n_{e(\text{fila})} = 7 \times 10^{19} \text{ m}^{-3}$, $B = 9.3 \text{ T}$, (b) $f = 4.6$ GHz (LH), $\lambda = 3.6$ mm, incident polarization: O-mode, $n_{e(\text{ambi})} = 2 \times 10^{19} \text{ m}^{-3}$, $n_{e(\text{fila})} = 4 \times 10^{19} \text{ m}^{-3}$, $B = 4.5 \text{ T}$, (c) $f = 170$ GHz (EC), $\lambda = 1.8$ mm, incident polarization: O-mode, $n_{e(\text{ambi})} = 10^{19} \text{ m}^{-3}$, $n_{e(\text{fila})} = 2 \times 10^{19} \text{ m}^{-3}$, $B = 5.4 \text{ T}$

Furthermore, in Figures 2a, 2b and 2c, one can see the results for the normalized radial stress for the three same cases of LH waves (radius $a = 2$ mm, 4 mm and 10 mm, respectively):

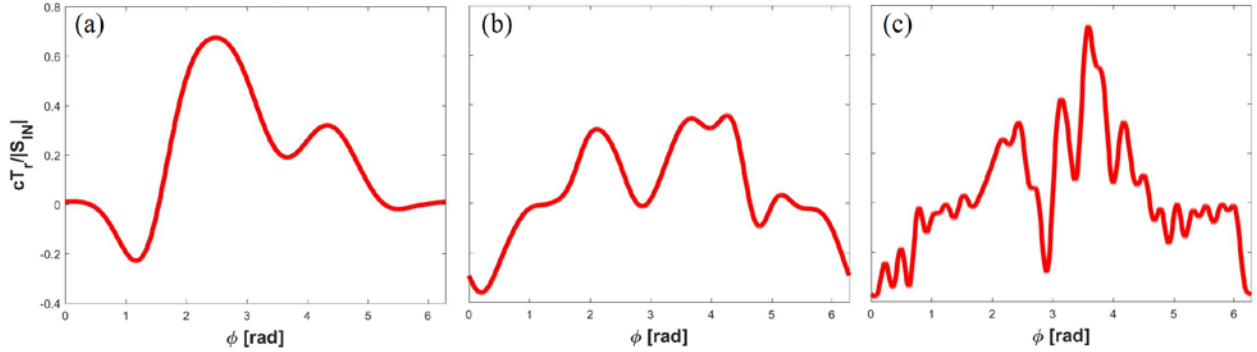


Figure 2: Normalized radial stress for the three same cases of LH waves (radius $a = 2$ mm, 4 mm and 10 mm)

The radial stress can be integrated from angle 0 to 2π so, that the force per unit axial length in x direction, per unit power flux can be calculated. The results are $7.60 \text{ (nN/m)/(kW/m}^2)$ for (a), $4.17 \text{ (nN/m)/(kW/m}^2)$ for (b) and $7.01 \text{ (nN/m)/(kW/m}^2)$ for (c). It is worth noting that the respective accelerations for power flux of 1 kW/m^2 attained by the filaments in (a), (b) and (c) are respectively about $461g$, $63g$ and $17g$ (g is the standard gravitational acceleration).

(d) Numerical Analysis

The ScaRF [4] Finite Difference Time Domain code has been developed for RF scattering in the plasma edge. It is a 3D full wave code capable of analysing scattering scenarios with arbitrary tensor permittivity (anisotropic) and plasma density profiles, for Bloch-periodic or non-periodic

boundary conditions. It has been used for the study of RF scattering from a periodic density fluctuation, (Figures 3a, 3b). In addition the ScaRF code has been applied in conjunction with the Polynomial Chaos Expansion-Smolyak Grid (PCE-SG) method for the Uncertainty Quantification of RF scattering from a more realistic, random harmonic interface (Figures 3b, 3c).

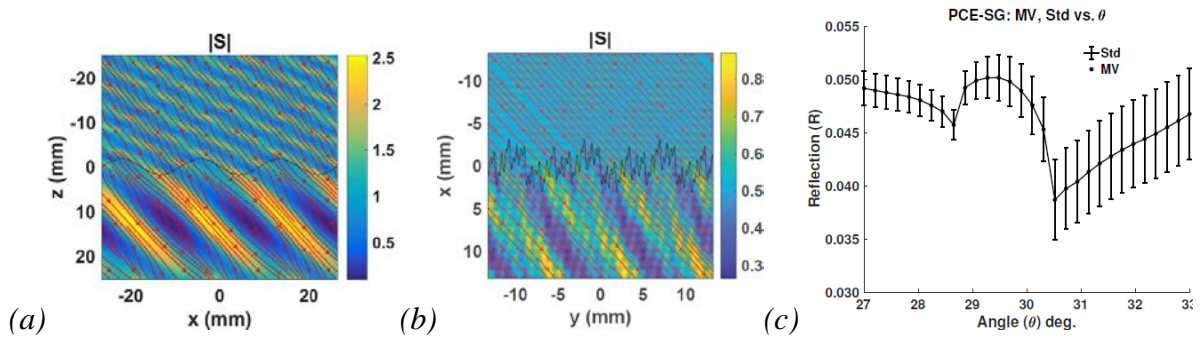


Figure 3: Poynting amplitude & Flux (red curves) for (a) periodic interface, (b) random interface (RI) with 5% variation in geometric parameters, (c) Mean Value (MV) and Standard Deviation (Std) of reflection in RI scattering, $f = 170$ GHz (EC), $\lambda = 1.9$ mm, incident polarization: O-mode, $n_{e(\text{ambi})} = 3 \times 10^{20} \text{ m}^{-3}$, $n_{e(\text{fila})} = 3.2 \times 10^{20} \text{ m}^{-3}$, $B = 4.5$ T

(e) Conclusions

The scattering of three different types of RF waves (IC, LH and EC) by turbulent cylindrical filament structures in the plasma edge was discussed for different filament radii. The results showed that by increasing the filament's radius, the scattering becomes more intense. Also, the forces exerted on the cylinder due to the incidence of RF waves, was studied. Furthermore, the ScaRF anisotropic code for 3D full wave scattering analysis was presented alone and in conjunction with the PCE-SG method, for random scattering scenarios.

References

- [1] A. K. Ram, K. Hizanidis and Y. Kominis, Physics of Plasmas 20, 056110 (2013)
- [2] A. K. Ram and K. Hizanidis, Physics of Plasmas 23, 022504 (2016)
- [3] S. I. Valvis, et al, Journal of Plasma Physics vol. 84, Issue 6, 745840604 (2018)
- [4] A. D. Papadopoulos, et al, Journal of Plasma Physics vol. 85, Issue 3, 905850309 (2019)
- [5] Z. C. Ioannidis, A. K. Ram, K. Hizanidis, and I. G. Tigelis, Physics of Plasmas 24, 102115 (2017)
- (*) S.I.V., A.D.P., K.H., P.P. and C.T. are partially supported by the Complementary Research Programme of the National Thermonuclear Fusion Research at NTUA. A.K.R. is supported by US DoE Grants DE-FG02-91ER54109 and DE-SC0018090.